# Supporting Information

## Enhanced photoelectrochemical performance from NiS-modified $TiO_2$ nanorods with surface charge accumulation facet

**Suyi Yang [a], Baoyuan Wang [a], Rui Zhao [a], Liting Wei [a], and Jinzhan Su [a*]**

[a]*International Research Center for Renewable Energy, State Key Laboratory of Multiphase Flow in Power Engineering, Xi'an Jiaotong University, Xi'an, Shaanxi 710049, People's Republic of China*

E-mail: j.su@mail.xjtu.edu.cn

*Corresponding author.
E-mail: j.su@mail.xjtu.edu.cn

### 1.1 Materials for the experiments

Fluorine-doped tin oxide substrates (FTO) coated glasses, acetone, ethanol, deionized water, acetylacetone, tetrabutyl titanate, hydrochloric acid, nickel chloride hexahydrate ($NiCl_2 \cdot 6H_2O$), sodium sul-fide hydrate ($Na_2S \cdot 9H_2O$), anhydrous sodium sulfate.

### 1.2 Preparation of $TiO_2$ seed layer by spin-coating method

Add 0.015M acetylacetone, 0.05M tetrabutyl titanate and 0.05M ethanol to 50ml deionised water to prepare the spin coating solution. A clean 1.5*3 cm FTO is fixed on the spin coater at 2000 rpm for 60 s and spin coated three times. After spin coating, the FTO is removed and heated at 60 °C for 10 minutes on a heating table. The sample was then transferred to a muffle furnace and annealed at 450 °C for 30 min. After cooling, the sample was removed and repeatedly rinsed with deionised water and heated on a heating table at 60 °C for 10 min.

### 1.3 Preparation of $TiO_2$ NRs

To 30 ml of deionised water add 30 ml of hydrochloric acid and 0.05 M tetrabutyl titanate. Transfer the FTO with the $TiO_2$ seed layer to the above solution, placing the side with the seed layer towards the bottom. Transfer to an oven and hold at 160 °C for 6 h. After completion of hydrothermal heating remove the FTO and wash repeatedly, dry by heating at 60 °C on a heating table and then transfer to a muffle furnace to anneal at 450 °C for 2 h [1].

### 1.4 Deposition of NiS on $TiO_2$ photoanode

Samples of the above prepared $TiO_2$ nanorod arrays were immersed in aqueous nickel chloride solution at a concentration of 0.01M, deionised water, aqueous sodium sulphide solution at 0.01M and deionised water, respectively, using the SILAR method [2]. Completion of one of these operations is counted as one continuous ion adsorption cycle, and one continuous ion adsorption cycle is dried on a heating table before the next continuous ion adsorption cycle. The work investigated different $TiO_2$/NiS nanorod arrays prepared by one, three and five sequential ion adsorption cycles, respectively, and the resulting samples were heated at 60 °C for 30 min on a heating table and transferred to a muffle furnace for annealing at 200 °C for 30 min.

### 1.5 Characterization

The scanning electron microscope (SEM, JEOL JSM-7800 F) and transmission electron microscopy (TEM, JEOL JEM-2100) were utilized to study the morphology of the prepared samples. An X-ray diffractometer (PANalytical X'pert PRO, Cu Kα irradiation (λ = 1.5418 Å)) was employed to study the crystal structure of the hybrid films. The chemical elements and states of the films were recorded with an X-ray photoelectron spectrometer (XPS, AXIS ULtrabld) using Al Ka (1486.6 eV) radiation as X-ray source and calibrated by C 1s (284.8 eV). A double-beam UV 4100 UV–vis-NIR spectrophotometer was used to investigate the UV–vis absorption spectra of the hybrid structure films. The PL spectra was obtained by using a FLS 980 fluorescence spectrophotometer at room temperature.

### 1.6 PEC measurements

The PEC measurements of photoanodes were performed using an electrochemical workstation (CHI 760E) in a standard three-electrode system. An as-obtained photoanode working electrode, a saturated Ag/AgCl reference electrode and a Pt foil counter electrode were used. A 0.5 M $Na_2SO_4$ buffer solution (pH = 6.8) was used as the electrolyte. The intensity density of simulated sunlight is controlled at 100 mW $cm^{-2}$ by a 350 W Xenon lamp with an AM 1.5 G filter. All photoanodes were illuminated by simulated sunlight through the sample side (i.e., a front illumination). On the other hand, the 808-nm NIR light comes from the back side of photoanodes. The tested area of the photoanode was about 0.196 $cm^2$. Current density-potential and linear sweep voltammograms measurements were performed using the scan rate of 20 mV $s^{-1}$. Faraday efficiency of $TiO_2$ and $TiO_2$/NiS-3 electrodes were performed in a closed cell with Ar-purge. The headspace in the cell was 30 mL and a constant current density of 0.6 -1.4 mA/$cm^2$ was applied for 60 min. The produced gas was determined by gas chromatography by taking 100 μL gas sample in the gas chamber, and then the Faraday efficiency was calculated according to Faraday's law.

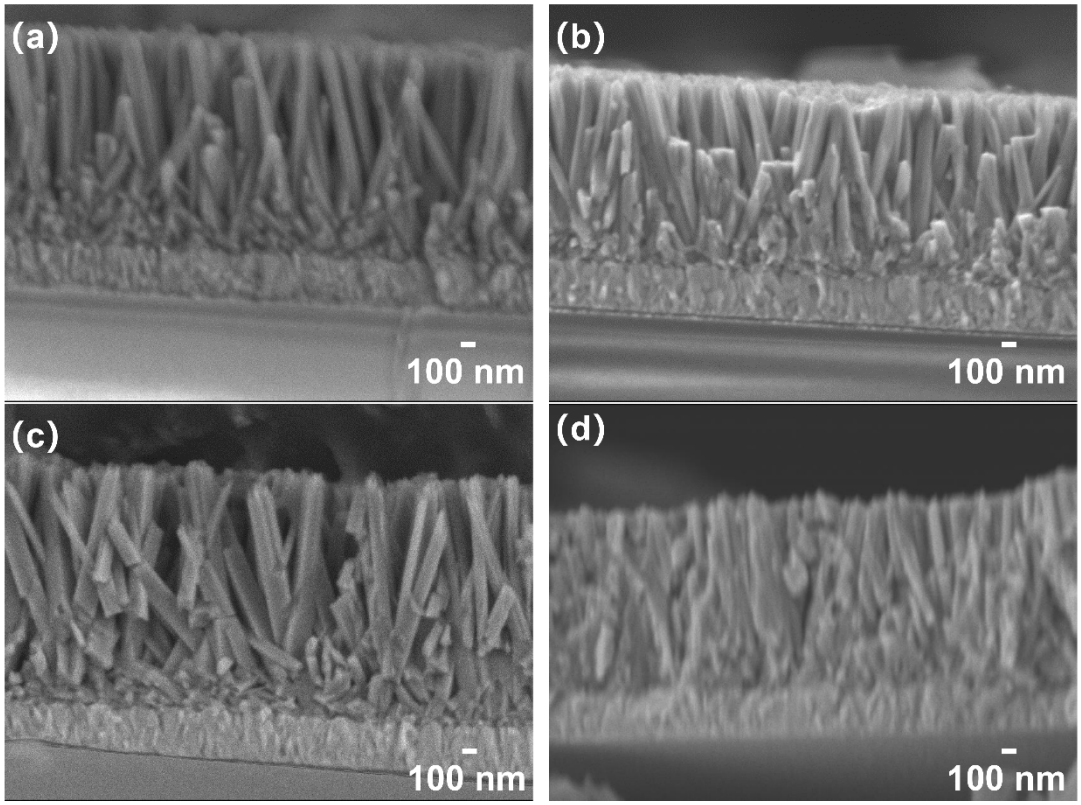


**Figure S1.** Cross-sectional SEM image of (a) pure $TiO_2$ NRs; (b) $TiO_2$/NiS-1; (c) $TiO_2$/NiS-3 and (d) $TiO_2$/NiS-5.

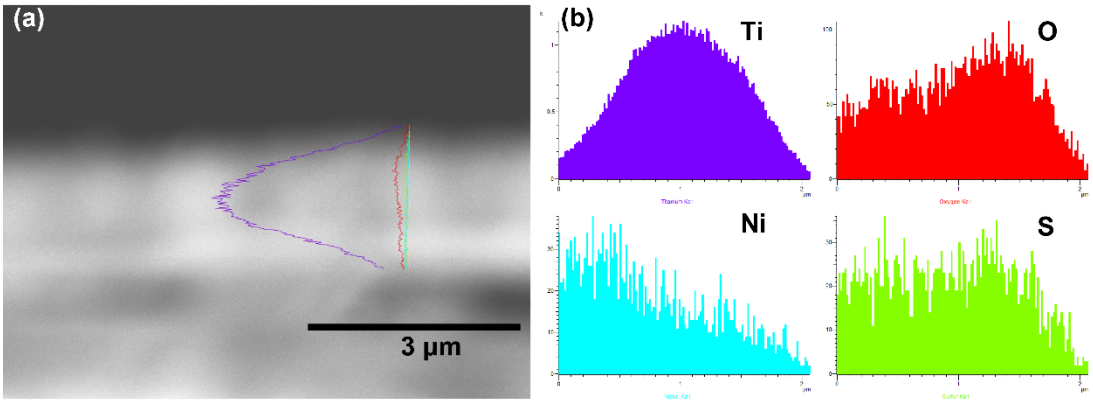


**Figure S2.** (a) Cross-sectional SEM image of $TiO_2$/NiS-3 composite, and (b) corresponding EDS line scan of Ti, O, Ni and S, respectively.

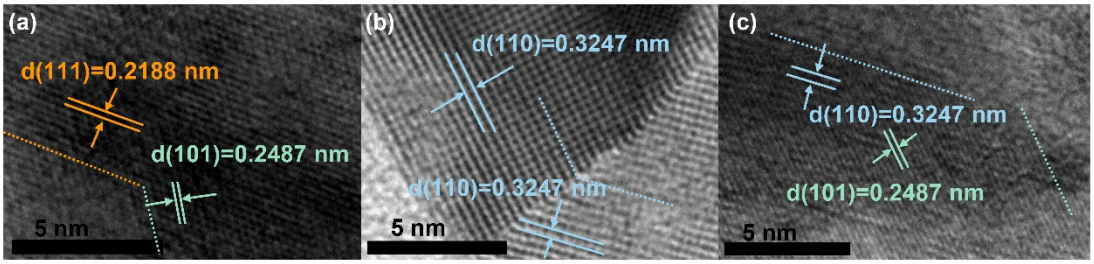


**Figure S3.**（a-c）HRTEM image of $TiO_2$.

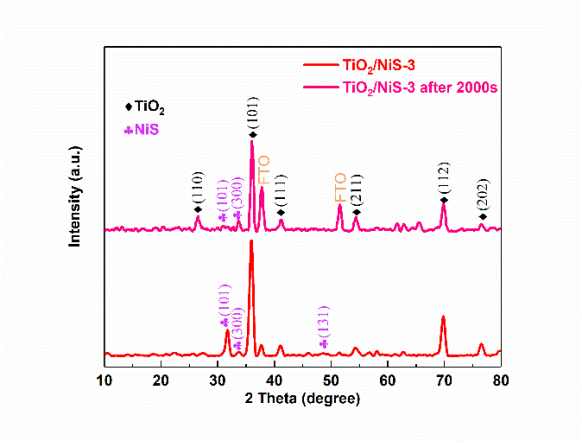


**Figure S4.** XRD patterns of bare $TiO_2$/NiS-3 NRs and $TiO_2$/NiS-3 after 2000 s.

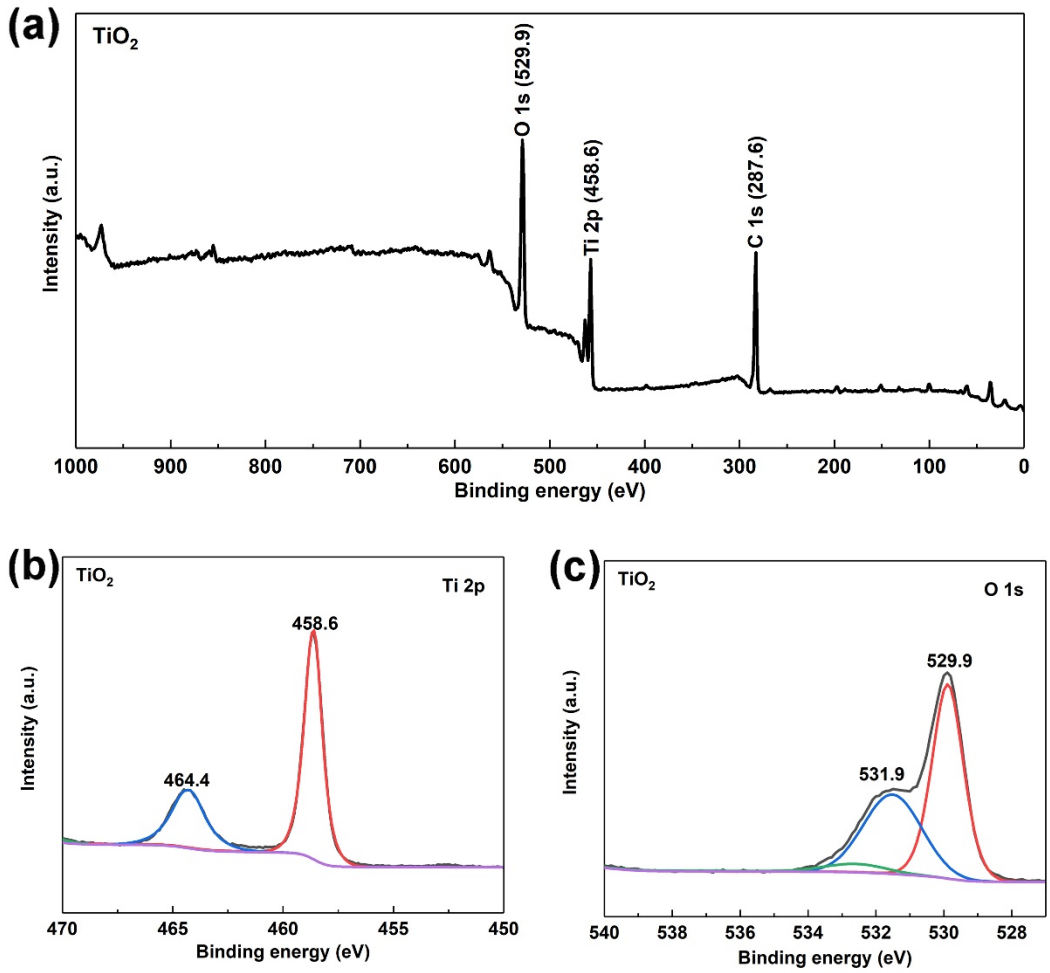


**Figure S5.** XPS spectra of $TiO_2$ nanostructure: (a) the survey spectrum; (b) Ti 2p peak; (c) O 1s peak.

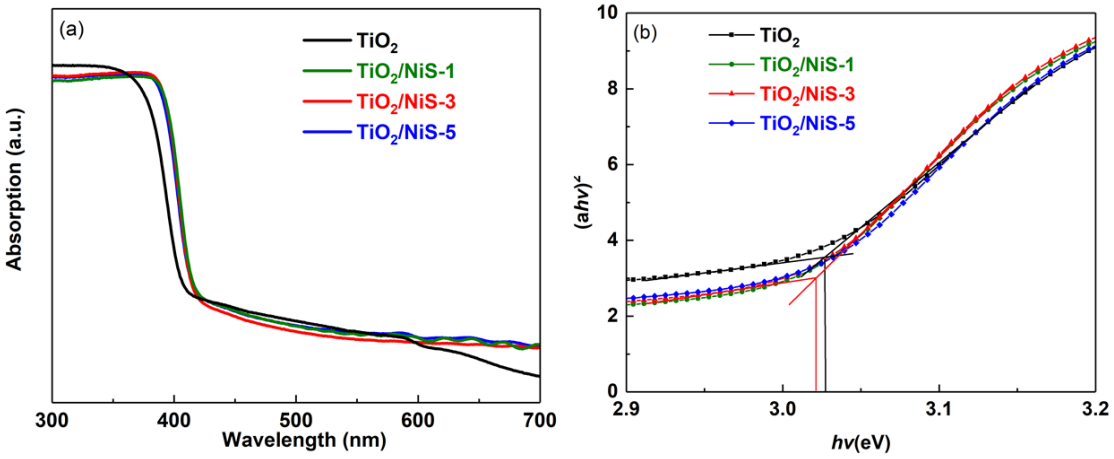


**Figure S6.** (a) UV–vis absorption spectra of $TiO_2$ and $TiO_2$/NiS-x ; (b) $(\alpha h\nu)^2$ versus photon energy spectra for $TiO_2$, and $TiO_2$/NiS-x nanorod arrays.

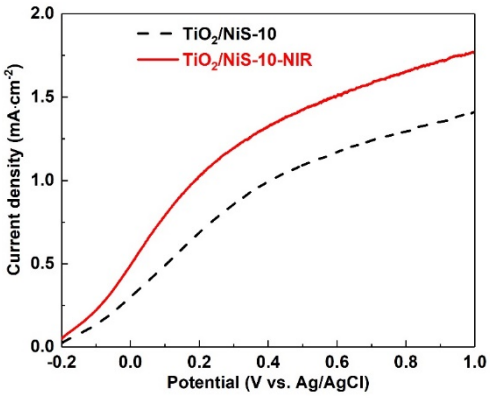


**Figure S7.** Photocurrent density-voltage curves of $TiO_2$/NiS-10 photoanodes under AM 1.5 G illumination with NIR light irradiation.

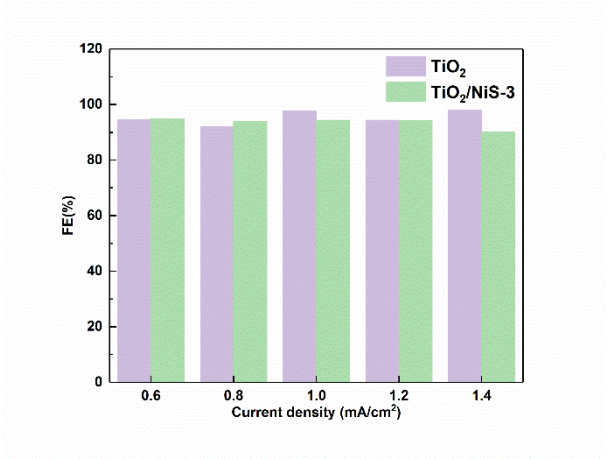


**Figure S8.** Faraday efficiency of $TiO_2$ and $TiO_2$/NiS-3 electrodes.

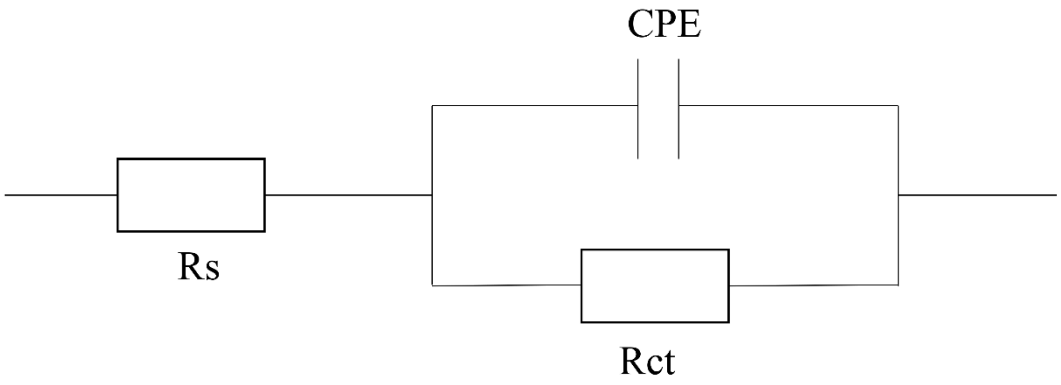


**Figure S9.** Simplified equivalent circuit used to fit EIS data in Nyquist plots.

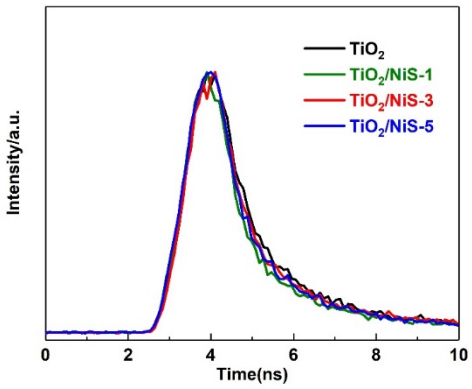


**Figure S10.** Time-resolved PL spectra of bare $TiO_2$ and $TiO_2$/NiS-x heterostructure.

**Table S1.** Water adsorption energies for different Rutile facets at 0 K [3]

| facets | molecular adsorption energy(eV) | dissociated adsorption energy(eV) |
|---|---|---|
| $TiO_2$(110) | -0.76 | -0.78 |
| $TiO_2$(101) | -1.18 | -1.16 |

**Table S2.** Fitted values of PL decay kinetics of pristine $TiO_2$ and $TiO_2$/NiS-x

| Sample | $B_1$ | $\tau_1$(ns) | $B_2$ | $\tau_2$(ns) | $\tau$ (ns) |
|---|---|---|---|---|---|
| $TiO_2$ | 2182.2 | 1.0516 | 226.7 | 5.2279 | 2.4738 |
| $TiO_2$/NiS-1 | 2132.5 | 0.8761 | 236.2 | 4.5225 | 2.2026 |
| $TiO_2$/NiS-3 | 1696.8 | 0.8162 | 312.3 | 4.1879 | 2.4540 |
| $TiO_2$/NiS-5 | 1890.7 | 0.8484 | 263.5 | 4.2677 | 2.2575 |

**Table S3.** Fitted values of EIS data of different samples.

| Sample | $R_s$(Ω) | CPE(μF) | $R_{ct}$(Ω) |
|---|---|---|---|
| $TiO_2$ | 71.8 | 4.4 | 8453 |
| $TiO_2$/NiS-1 | 84.5 | 12.6 | 4045 |
| $TiO_2$/NiS-3 | 112.3 | 15.3 | 1163 |
| $TiO_2$/NiS-5 | 71.2 | 26.1 | 3850 |

(1) Li, X.; Zhang, T.; Chen, Y.; Fu, Y.; Su, J.; Guo, L. Hybrid nanostructured Copper(II) phthalocyanine/$TiO_2$ films with efficient photoelectrochemical performance. *Chemical Engineering*

*Journal* **2020**, *382*. DOI: 10.1016/j.cej.2019.122783.

(2) Chen, D.; Liu, Z.; Guo, Z.; Yan, W.; Ruan, M. Decorating Cu2O photocathode with noble-metal-free Al and NiS cocatalysts for efficient photoelectrochemical water splitting by light harvesting management and charge separation design. *Chemical Engineering Journal* **2020**, *381*. DOI: 10.1016/j.cej.2019.122655.

(3) Kamphaus, E. P.; Shan, N.; Jones, J. C.; Martinson, A. B. F.; Cheng, L. Selective Hydration of Rutile TiO2 as a Strategy for Site-Selective Atomic Layer Deposition. *ACS Appl Mater Interfaces* **2022**, *14* (18), 21585-21595. DOI: 10.1021/acsami.1c24807.